

# Closed loop inner current control of Grid Connected MMC based microgrid solar system in dq Frame

1<sup>st</sup> WIAM HERKAT  
dept.Power and Control  
university of Boumerdes (UMBB)  
Algeria  
w.herkat@univ-boumerdes.dz

2<sup>nd</sup> YASSINE YAKHELEF  
dept.Power and Control  
university of Boumerdes (UMBB)  
Algeria  
y.yakhelef@univ-boumerdes.dz

**Abstract**—The microgrid solar system integrates renewable energy sources, such as solar photovoltaic panels, into the grid through an MMC, enabling efficient and reliable power conversion. The inner current control strategy is critical for maintaining the stability and performance of the microgrid under varying operating conditions. In this paper, we present a comprehensive study on the closed-loop inner current control of a Grid-Connected Modular Multilevel Converter (MMC) based microgrid solar system, employing the dq (direct-quadrature) frame for control reference. It will elaborate on the design and implementation of the closed-loop inner current control system, discussing the selection of control method and appropriate control parameters. The control scheme's effectiveness is evaluated through extensive simulation studies.

**Index Terms**—Modular multilevel Converter(MMC), PV system grid-connected, current control.

## I. INTRODUCTION

The integration of renewable energy sources and the demand for efficient power transmission have led to the widespread adoption of Modular Multilevel Converters (MMCs) in modern power systems. [1] [2] [3]

Modular Multilevel converters offer several advantages, including high modularity and scalability, allowing for easy expansion or modification of the system. Additionally, its ability to tolerate faults within individual submodules enhances the system's reliability. Overall, the MMC circuit has proven to be a versatile and efficient solution for applications such as high-voltage direct current (HVDC) transmission and renewable energy integration. [4] Their modular design allows for scalability, ensuring the adaptation to a wide range of power requirements. With high efficiency and low harmonic generation, MMCs minimize energy losses during the conversion process; additionally, their modularity allows for flexible and adaptable control strategies that can be customized to suit different applications and operating conditions [4].

The paper's structure is outlined as follows: in section I we present a concise introduction to the MMC converter; section II focuses on establishing a mathematical model for the MMC; in Section III, we establish a control strategy for inner currents; a simulation is conducted in section IV and performance of the proposed controller is investigated. Finally, the conclusion is provided in section V.

## II. MMC MATHEMATIC MODEL

1) *circuit configuration* : The MMC circuit is an advanced voltage source converter, which utilizes multiple submodules (SMs) interconnected in a specific configuration. Each submodule

consists of a series-connected set of semiconductor switches (typically insulated gate bipolar transistors, IGBTs) and capacitors. These submodules are arranged in arms, often in a symmetrical fashion to ensure balanced operation. The arms are connected in parallel and are controlled independently to achieve the desired output voltage waveform.

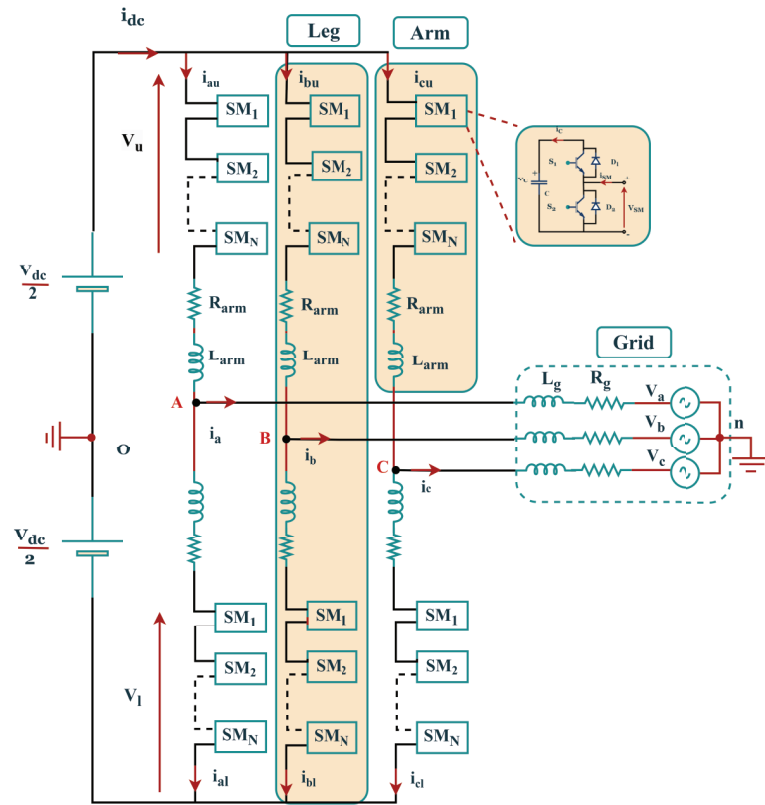


Fig. 1: Circuit diagram for MMC

Each sub module is controlled separately where the individual voltages  $V_{SM}$  add up to form a multilevel, nearly sinusoidal staircases waveform [5]

The dynamic equations used for the submodule capacitor voltages are provided by

$$C \frac{V_{SMu}}{dt} = i_{au} S_j \quad (1)$$

$$C \frac{V_{SMl}}{dt} = i_{al} S_j \quad (2)$$

$V_{dc}$	Dc bus voltage
$i_{dc}$	DC bus current
$i_u$	upper arm current
$i_l$	lower arm current
$i_{zj}$	AC circulating current
$i_{comm}$	common mode current
$i_{diff}$	differential current
$i_g$	Grid current
$i_{oj}$	Phase output current
$i_{SM}$	Submodule current
$V_g$	Grid voltage
$V_c$	Capacitor voltage
$V_{SM}$	Submodule Output Voltage
$V_{uj}$	upper arm voltage of the phase j
$V_{lj}$	lower arm voltage of the phase j
$V_{oj}$	Inverter output voltage
$V_{diff}$	differential voltage
$L$	Arm inductor
$R$	Arm resistance
$L_g$	Grid inductor
$R_g$	Grid resistance
$C$	Submodule Capacitor

TABLE I: the parameters of MMC

$S_1$	$S_2$	$V_{SM}$	Capacitor
ON	OFF	$V_c$	Charging
OFF	ON	0	Uncharged

TABLE II: Switching States of SM

where  $S_j = 1$  when submodule is ON and  $S_j = 0$  when Submodule is OFF. Modular Multilevel Converter is mainly composed of  $N$  identical submodules per arm that are connected in series. The MMC circuit consists of multiple arms, typically six, for a three-phase system. Each arm is responsible for generating a portion of the output voltage.

**Submodules (SMs):** Within each arm, multiple submodules are connected in series. The number of SMs per arm can vary based on the desired voltage and power levels. Each submodule contains switching devices, typically Insulated Gate Bipolar Transistors (IGBTs), for controlling current and voltage.

**DC Capacitors:** Each submodule contains a DC capacitor. These capacitors store and provide energy, ensuring that the output voltage remains stable. [6]

Considering a phase circuit of MMC to simplify the model, each arm will be represented by a voltage source in series with the arm inductance and resistance where,

a specific SM configuration can improve the performance of an MMC in terms of power flow control and fault tolerance, without significantly increasing its cost or complexity. The best balance between complexity and functionality can be found in bipolar configurations like the SC-SM and CD SM, though the HB-SM is still an option if negative voltage levels are not required. [7]

circulating current equations [8]

Using Kirchhoff voltage law (KVL), the dynamics of the MMC is defined by the following equations:

$$\frac{V_{dc}}{2} - V_{uj} - V_g = (Ri_{uj} + L \frac{di_{uj}}{dt}) + (R_g i_{oj} + L_g \frac{di_g}{dt}) \quad (3)$$

$$-\frac{V_{dc}}{2} + V_{lj} - V_{oj} = -(Ri_{lj} + L \frac{di_{lj}}{dt}) + (R_g i_{oj} + L_g \frac{di_g}{dt}) \quad (4)$$

the upper and the lower arm voltages depend on the state of the switches and also the voltage of the capacitors of the modules

$$V_{uj} = \sum_{n=1}^k S_{ujn} \cdot V_{cujn} \quad (5)$$

$$V_{lj} = \sum_{n=1}^k S_{ljn} \cdot V_{cljn} \quad (6)$$

by defining the phase current  $i_{oj}$  and the circulating current  $i_{zj}$ , where  $j$  refers to the three phases of MMC (a, b, and c)

$$i_{zj} = \frac{i_{uj} + i_{lj}}{2} \quad (7)$$

$$i_{oj} = i_{uj} - i_{lj} \quad (8)$$

The upper and lower arm currents can be expressed by:

$$i_{uj} = i_{zj} + \frac{i_{oj}}{2} \quad (9)$$

$$i_{lj} = i_{zj} - \frac{i_{oj}}{2} \quad (10)$$

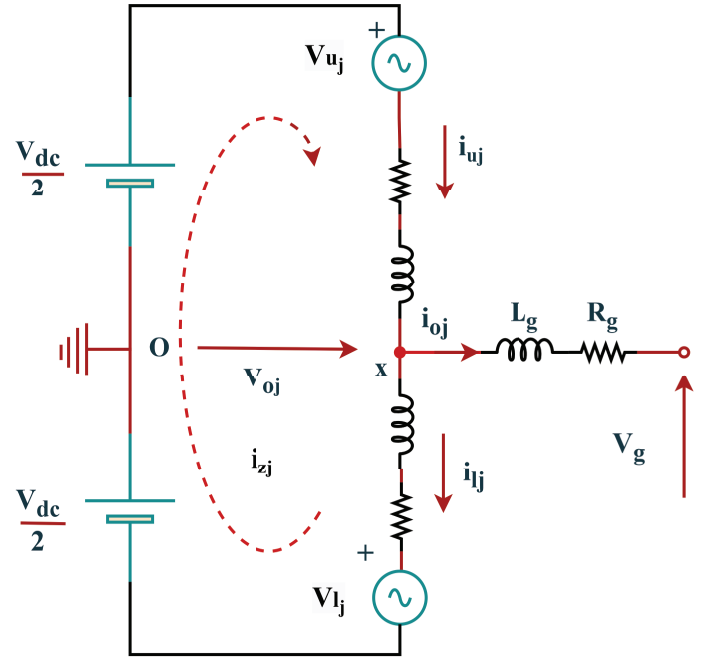


Fig. 2: Single-phase equivalent circuit of the 3Ph MMC

the equations 3 and 4 can be written as follows:

$$V_{oj} = \frac{V_{up} - V_{low}}{2} - \frac{L}{2} \frac{di_{xi}}{dt} - \frac{R}{2} i_{xi} \quad (11)$$

$$2L \frac{di_{zj}}{dt} - 2R i_{zj} = V_{dc} - (V_{uj} + V_{lj}) \quad (12)$$

$$V_{diff} = \frac{V_u - V_l}{2} \quad (13)$$

In the MMC, the common mode current and differential current are expressed by:

$$i_{comm} = \frac{i_u - i_l}{2} \quad (14)$$

$$i_{diff} = \frac{i_u - i_l}{2} \quad (15)$$

$$i_{uj} = \frac{i_a}{2} + i_{diff} \quad (16)$$

$$i_{lj} = \frac{i_a}{2} - i_{diff} \quad (17)$$

2) *MMC model in dq frame*: The following system dynamics in dq-frame are obtained by applying the standard abc/dq transformation to (3). [9]

$$L \begin{bmatrix} \frac{di_d}{dt} \\ \frac{di_q}{dt} \end{bmatrix} = \begin{bmatrix} u_d \\ u_q \end{bmatrix} - \begin{bmatrix} R & \omega L \\ \omega L & R \end{bmatrix} \begin{bmatrix} i_d \\ i_q \end{bmatrix} - \begin{bmatrix} e_d \\ e_q \end{bmatrix}$$

where  $e_d, e_q$  are the grid voltages in dq frame

As indicated in the previous equation, the system dynamics in the dq-frame exhibit significant coupling. To mitigate this coupling, the decoupling control scheme illustrated in Figure 4 is applied in the following manner.

$$\begin{bmatrix} u_d \\ u_q \end{bmatrix} = \begin{bmatrix} -\omega L & 1 \\ 1 & \omega L \end{bmatrix} \begin{bmatrix} i_d \\ i_q \end{bmatrix} + \begin{bmatrix} e_d \\ e_q \end{bmatrix} + \begin{bmatrix} u_{id} \\ u_{iq} \end{bmatrix}$$

where  $u_{id}, u_{iq}$  are the control output from the PI controller

### III. OVERALL MMC CONTROL

As indicated in equation (20), the system dynamics in the dq-frame exhibit significant coupling. To mitigate this coupling, the decoupling control scheme illustrated in Figure 2 is applied in the following manner. MMC control diagram consists of various

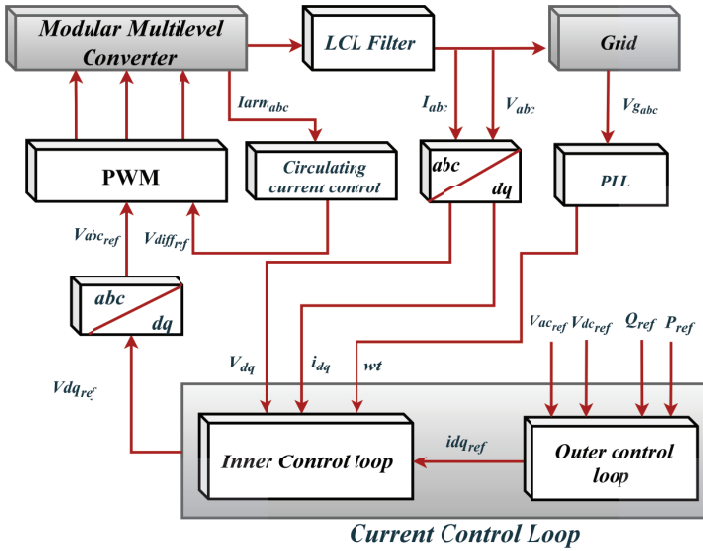


Fig. 3: Control Diagram of MMC

control loops and signal processing elements like filters, d-q axis transformations, and a phase-locked loop (PLL). The main control loops include AC current control and leg current control. [10] When it comes to inverters with multi-variable control, cascaded current-voltage control is utilized. This control consists of an inner voltage loop and an outer current loop. By introducing multiple feedback variables [11], the controller becomes more

flexible and improves the power quality of both the local load voltage and the current exchanged with the grid [12].

the inner control loop generates the reference voltage signal using decoupling current control and voltage feed forward control [13] while The outer control loop sets the desired power exchange between the MMC and the grid. It calculates the reference power values based on grid requirements, system load, or other control objectives. [14] The outer-loop control provides a total of three distinct control modes: active/reactive power control, DC voltage control, and AC voltage control. [15]

The choice of power converter control and modulation techniques for an MMC depends on the specific applications in which it is utilized. To illustrate, solar photovoltaic (PV) systems often make use of sinusoidal pulse width modulation (SPWM) techniques coupled with proportional integral control [16]

The LCL filter plays a crucial role in improving the current quality. It effectively reduces high-frequency harmonics and decreases the ripple caused by switching frequencies in the current waveform [17] Phase-Shifted PWM is a modulation technique that involves generating multiple PWM signals with controlled phase offsets when MMC is operating under unbalanced voltage

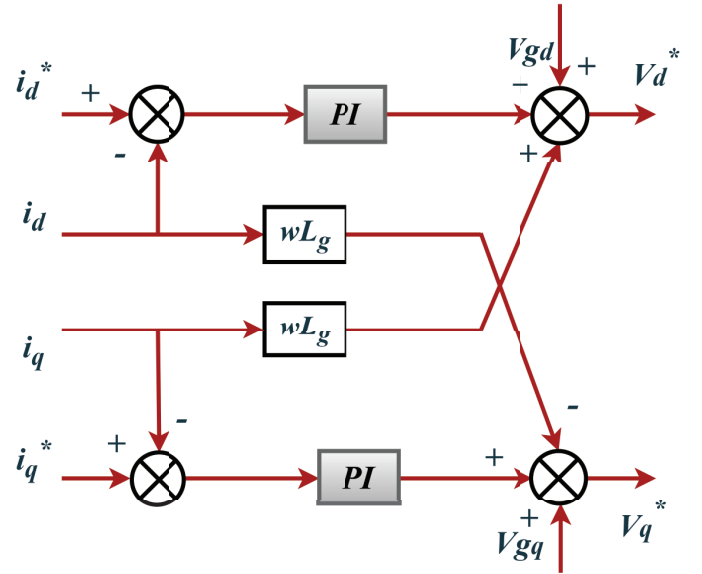


Fig. 4: Inner control loop

conditions, there are additional components, including positive-sequence and zero-sequence circulating currents [18] a dual-vector current controller is proposed to reduce AC-side active power ripple when unbalanced voltages .it also introduces a control approach that accounts for all components of circulating currents under such conditions.

### IV. SIMULATION RESULTS

The proposed control technique aims to regulate the power flow and and control the output current and ensure stability in the three-phase Modular Multilevel converter, Matlab/Simulink software is used to create a three-phase MMC inverter with a resistor-inductor load in order to validate the suggested control scheme.

The diagram of the circulating current in Figure 5 shows that the circulating current is very much like a pure direct current (dc).the circulating current is approaching zero, indicating a balanced condition.In summary, a circulating current plot signifies

a well-controlled and balanced operation, contributing to system stability and efficiency.

As shown in Figure 6 ,before using PI controller the output voltage signal exhibit irregularities and distortions furthermore the absence of precise control mechanisms that lead to deviations from the desired sinusoidal waveform, resulting in higher Total Harmonic Distortion (THD) levels.however after control, lower THD levels are noticed compared to the uncontrolled state, thereby improving the overall quality of the output voltage signal which emphasizes the effectiveness of the controller.

At the same time, Figure 7(a) and (b) show the results obtained by using PI controller ,a more balanced output current is noticed and the waveform looks almost exactly like a smooth, pure sine wave with very little distortion.

The FFT Analysis of the output voltage and output current are illustrated in Figure 8 and Figure 9 respectively ,the introduction of PI control helped in reducing harmonic distortions in the output voltage and current waveform.which demonstrates the effectiveness of the control strategy in improving the power quality of the MMC's outputs.

Parameter	Symbol	Value
Number of submodules	$N$	4
Switching frequency	$F_s$	5000Hz
Nominal Frequency	$f$	50Hz
Angular frequency -	$w$	$2 * \pi * f$
AC System voltage	$V_{AC}$	8KV
Filter inductor	$L_g$	0.004H
Filter capacitor	$C_g$	1 $\mu$ F
Submodule capacitance	$C$	1000 $\mu$ F
Arm inductance	$L_{arm}$	0.004H
Arm resistance	$R_{arm}$	0.1ohm
Dc bus voltage	$V_{dc}$	35.36e + 3V

TABLE III: Simulation parameters of three phase MMC

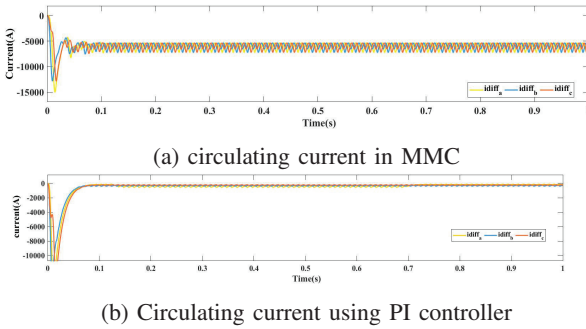


Fig. 5: Comparison of Circulating Current: Pre and Post Control

## V. CONCLUSION

Future investigations in the control of Modular Multilevel Converters MMC are likely to focus on several key areas including the development of more sophisticated control algorithms to enhance the performance of MMC, this could involve the use of artificial intelligence, machine learning, and predictive control methods to improve the converter's dynamic response and efficiency furthermore research on how MMC can contribute to grid stability and integration of renewable energy sources

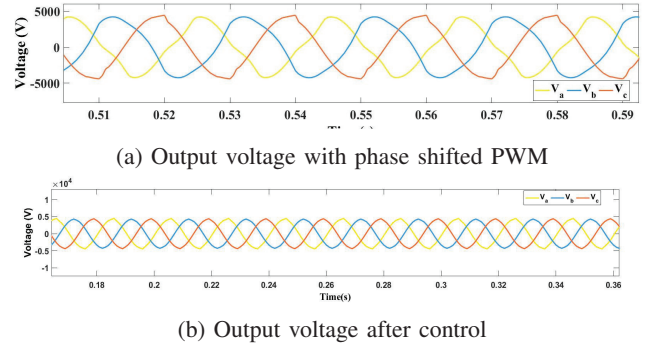


Fig. 6: Converter output voltage before and after control

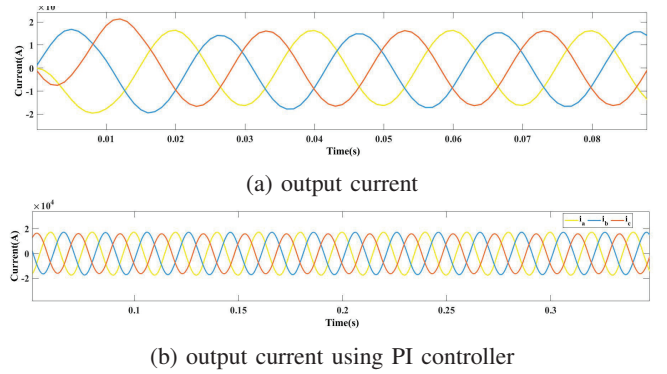


Fig. 7: Comparison of output Current: Pre and Post Control

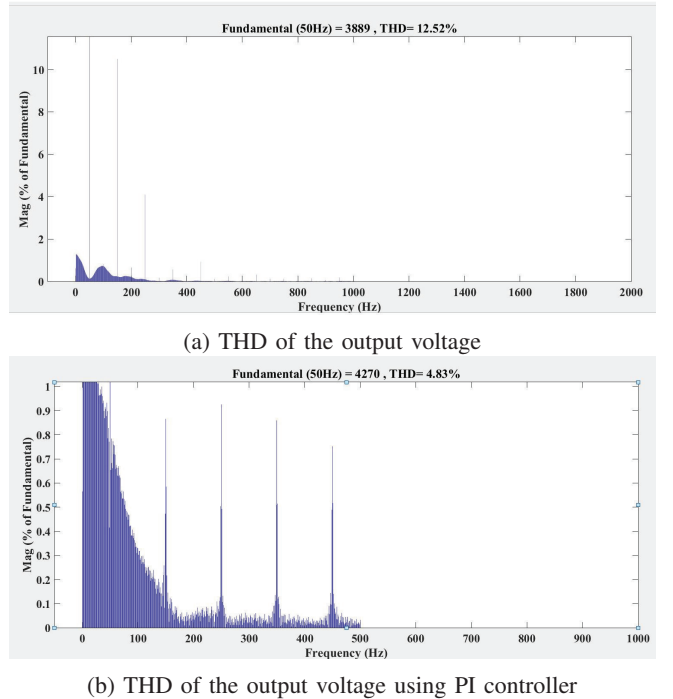
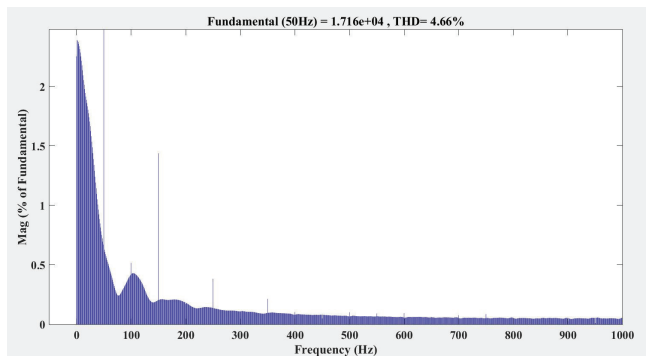
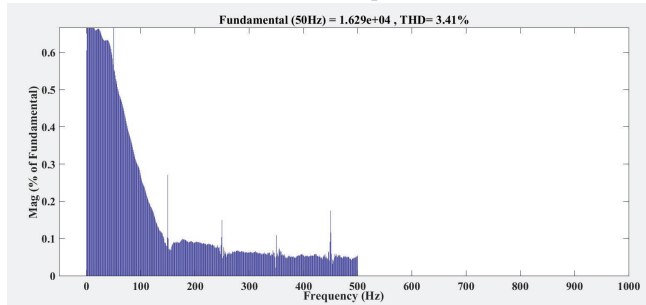


Fig. 8: Comparison of output voltage THD Pre and Post Control





(a) THD of the output current



(b) THD of the output current using PI controller

Fig. 9: Comparison FFT analysis of output current Pre and Post Control

## REFERENCES

- [1] J. Rodriguez, L. G. Franquelo, S. Kouro, J. I. Leon, R. C. Portillo, M. A. M. Prats, and M. A. Perez, "Multilevel converters: An enabling technology for high-power applications," *Proceedings of the IEEE*, vol. 97, no. 11, pp. 1786–1817, 2009.
- [2] R. Marquardt, "Modular multilevel converters: State of the art and future progress," *IEEE Power Electronics Magazine*, vol. 5, no. 4, pp. 24–31, 2018.
- [3] A. A. Mahmoud, A. A. Hafez, and A. M. Yousef, "Modular multilevel converters for renewable energies interfacing: Comparative review," in *2019 IEEE Conference on Power Electronics and Renewable Energy (CPERE)*. IEEE, 2019, pp. 397–406.
- [4] M. Kurtoğlu, F. Eroğlu, A. O. Arslan, and A. M. Vural, "Recent contributions and future prospects of the modular multilevel converters: A comprehensive review," *International Transactions on Electrical Energy Systems*, vol. 29, no. 3, p. e2763, 2019.
- [5] U. N. Gnanarathna, A. M. Gole, and R. P. Jayasinghe, "Efficient modeling of modular multilevel hvdc converters (mmc) on electromagnetic transient simulation programs," *IEEE Transactions on power delivery*, vol. 26, no. 1, pp. 316–324, 2010.
- [6] L. Harnefors, A. Antonopoulos, S. Norrga, L. Angquist, and H.-P. Nee, "Dynamic analysis of modular multilevel converters," *IEEE Transactions on Industrial Electronics*, vol. 60, no. 7, pp. 2526–2537, 2012.
- [7] G. Konstantinou, J. Zhang, S. Ceballos, J. Pou, and V. G. Agelidis, "Comparison and evaluation of sub-module configurations in modular multilevel converters," in *2015 IEEE 11th International Conference on Power Electronics and Drive Systems*. IEEE, 2015, pp. 958–963.
- [8] A. Marzoughi, R. Burgos, D. Boroyevich, and Y. Xue, "Steady-state analysis of voltages and currents in modular multilevel converter based on average model," in *2015 IEEE Energy Conversion Congress and Exposition (ECCE)*. IEEE, 2015, pp. 3522–3528.
- [9] M. Alqatamin, J. Latham, Z. T. Smith, B. M. Grainger, and M. L. McIntyre, "Current control of a three-phase, grid-connected inverter in the presence of unknown grid parameters without a phase-locked loop," *IEEE Journal of Emerging and Selected Topics in Power Electronics*, vol. 9, no. 3, pp. 3127–3136, 2020.
- [10] P. Bordignon, M. Marchesoni, G. Parodi, and L. Vaccaro, "Modular multilevel converter in hvdc systems under fault conditions," in *2013 15th European Conference on Power Electronics and Applications (EPE)*. IEEE, 2013, pp. 1–10.
- [11] Q. Liu, T. Caldognetto, and S. Buso, "Review and comparison of grid-tied inverter controllers in microgrids," *IEEE Transactions on Power Electronics*, vol. 35, no. 7, pp. 7624–7639, 2019.

- [12] Q.-C. Zhong and T. Hornik, "Cascaded current–voltage control to improve the power quality for a grid-connected inverter with a local load," *IEEE Transactions on Industrial Electronics*, vol. 60, no. 4, pp. 1344–1355, 2012.
- [13] X. Zhou, Y. Zhou, Y. Ma, L. Yang, X. Yang, and B. Zhang, "Dc bus voltage control of grid-side converter in permanent magnet synchronous generator based on improved second-order linear active disturbance rejection control," *Energies*, vol. 13, no. 18, p. 4592, 2020.
- [14] Y. Zhang, J. Ravishankar, and R. Li, "Modelling and control of modular multi-level converter based hvdc systems using symmetrical components," in *2015 IEEE 15th International Conference on Environment and Electrical Engineering (EEEIC)*. IEEE, 2015, pp. 1910–1915.
- [15] T. Yin, Y. Wang, X. Wang, B. Yue, D. Zhao, J. Sun, P. Li, and Y. Liu, "Modeling and analysis of high-frequency mmc impedance considering different control modes and voltage feedforward," *IEEE Access*, vol. 8, pp. 218 575–218 584, 2020.
- [16] S. Alotaibi and A. Darwish, "Modular multilevel converters for large-scale grid-connected photovoltaic systems: A review," *Energies*, vol. 14, no. 19, p. 6213, 2021.
- [17] M. Liserre, F. Blaabjerg, and S. Hansen, "Design and control of an lcl-filter-based three-phase active rectifier," *IEEE Transactions on industry applications*, vol. 41, no. 5, pp. 1281–1291, 2005.
- [18] W.-S. Do, S.-H. Kim, T.-J. Kim, and R.-Y. Kim, "A study of circulating current in mmc based hvdc system under an unbalanced grid condition," in *IECON 2014-40th Annual Conference of the IEEE Industrial Electronics Society*. IEEE, 2014, pp. 4146–4152.